for hospitality to W.A.F. during his sabbatical leave, Dr. A. Annamalai and M. P. Fearon for help in checking experimental data, and Prof. John Morrison for helpful discussions.

Registry No. I, 696-75-3; (-)-1*R*,2*R*-I, 34202-45-4; II, 86022-60-8; (+)II, 85976-95-0; III, 2345-75-7.

Supplementary Material Available: Tables of anisotropic thermal parameters for the non-hydrogen atoms and isotropic thermal parameters for the hydrogen atoms, bond angles involving hydrogen atoms, and observed and calculated structure factors and a stereoview of the unit cell (11 pages). Ordering information is given on any current masthead page.

Contribution from the Department of Chemistry, University of California, Los Angeles, California 90024, Istituto di Chimica Analitica, Universita di Sassari, 01700 Sassari, Italy, Istituto di Chimica Generale, Universita di Milano, 20133 Milano, Italy, and Istituto Chimico, Universita di Camerino, 62032 Camerino, Italy

Synthesis and Characterization of Dinuclear Trihydride Complexes of Platinum with Chelating Ligands. Crystal and Molecular Structure of $[Pt_2H_3(Ph_2P(CH_2)_2PPh_2)_2][BPh_4]$

CAROLYN B. KNOBLER,*[1a] HERBERT D. KAESZ,*[1a] GIOVANNI MINGHETTI,*[1b] ANNA LAURA BANDINI,[1c] GUIDO BANDITELLI,[1c] and FLAVIO BONATI*[1d]

Received August 18, 1982

A series of cationic dinuclear trihydride complexes of platinum have been prepared and isolated as the different salts $[Pt_2H_3(L\text{-}L)_2][A]$: **1a**, L-L = $Ph_2P(CH_2)_2PPh_2$ (dpe), A = BF_4; **1b**, L-L = dpe, A = I; **1c**, L-L = dpe, A = NO_3; **1d**, L-L = dpe, A = BPh_4; **1a-d_3**, L-L = dpe, A = BF_4; **2a**, L-L = $Ph_2P(CH_2)_3PPh_2$ (dpp), A = BF_4; **3a**, L-L = $Ph_2P(CH_2)_4PPh_2$ (dpb), A = BF_4; **3c**, L-L = dpb, A = NO_3; **4a**, L-L = *cis*-$Ph_2PCH{=}CHPPh_2$ (dpet), A = BF_4; **5a**, L-L = $Ph_2P(CH_2)_2AsPh_2$ (dpae), A = BF_4. Raman spectroscopic data (for **1a**) indicate the presence of both terminally bonded and bridge-bonded hydride while only the terminal hydride absorptions are seen in the IR spectra. ^1H, ^{31}P, and ^{195}Pt NMR studies indicate fluxional behavior down to -95 °C. Crystal and molecular structure determination of **1d** was undertaken at 115 K. The salt crystallizes in the monoclinic space group C_{2h}^5-$P2_1/n$ with cell dimensions a = 11.107 (2) Å, b = 29.118 (4) Å, c = 19.646 (2) Å, and β = 97.62 (1)°. There are four $[Pt_2H_3Ph_2P(CH_2)_2PPh_2]$ cations and four BPh_4 anions per unit cell. The bidentate phosphine groups are chelated each to a separate metal atom, and two hydrogen atoms are observed to be bridging between the two metal atoms. If the bridging hydrogen atoms are ignored, coordination around one of the two metal atoms, Pt(1), is close to a square plane while that around Pt(2) is trigonal. The square plane around Pt(1) consists of two cis-coordinated phosphorus atoms, Pt(2), and the terminally bonded hydrogen atom. The trigonal coordination around Pt(2) is composed of two cis-coordinated phosphorus atoms and Pt(1). The Pt-Pt distance (bridged by two hydrogen atoms) is 2.728 Å with Pt-H_μ distances estimated to be in the range 1.4 (1)-2.0 (1) Å.

Introduction

The chemistry of the platinum hydrides has been almost completely dominated for many years by mononuclear species of the types *trans*-$[Pt(H)(PR_3)_2(L)]^{n+}$ (n = 1, L = neutral ligand; n = 0, L = anionic ligand)[2] and and *trans*-$[Pt(H)_2(Pr'_3)_2]$, where R' is a bulky substituent.[3] *cis*-Dihydride complexes with chelating ligands were reported first in 1976 by Shaw et al.[4] and later by Otsuka, Ibers, and co-workers.[5]

Dinuclear species were unknown until the same year, when the neutral species $[Pt_2(X)_2(\mu\text{-}H)_2(L)_2]$ (L = $P(C_6H_{11})_3$; X = H, SiR_3, GeR_3) were described by Stone et al.[6] In 1977, two reports, one by members of our group[7] and the other by Brown, Puddephatt, et al.,[8] gave account of the isolation of the cations $[Pt_2H_3(dpe)_2]^+$, dpe = $Ph_2P(CH_2)_2PPh_2$, and $[Pt_2H_2(\mu\text{-}H)(\mu\text{-}dpm)_2]^+$, dpm = $Ph_2PCH_2PPh_2$, respectively. Since then, several other papers have described complexes containing the $Pt_2H_3P_4$ unit[9,10] as well as different aspects of their reactivity.[11-14] Dinuclear cationic complexes are seen to derive from mononuclear Pt(II) complexes in reactions of the type shown in Scheme I. These reactions involve the displacement by PtH_2L_2 of X^- or solvent (S) on $Pt(H)XL_2$[10] or $[Pt(H)(S)L_2]^+$.[9c] These derivatives may also be considered to arise from the oxidative addition of PtH_2L_2 at a Pt^0L_2 center, followed by protonation, indicated in eq 3 of Scheme I. Some of the dinuclear species are known to be fluxional,[7,8,10] and the structure for the salt of $[Pt_2H_3(L\text{-}L)_2]^+$, L-L = $(t\text{-}Bu)_2P(CH_2)_3P(t\text{-}Bu)_2$, has been determined.[10]

(1) (a) University of California. (b) Universita di Sassari. (c) Universita di Milano. (d) Universita di Camerino.
(2) Hartley, F. R. "The Chemistry of Platinum and Palladium"; Wiley: New York, 1973.
(3) (a) Shaw, B. L.; Uttley, M. F. *J. Chem. Soc., Chem. Commun.* **1974**, 918. (b) Green, M.; Howard, J. A.; Spencer, J. L.; Stone, F. G. A. *Ibid.* **1975**, 3. (c) Immirzi, A.; Musco, A.; Carturan, G.; Belluco, U. *Inorg. Chim. Acta* **1975**, *12*, L23. (d) Yoshida, T.; Otsuka, S. *J. Am. Chem. Soc.* **1977**, *99*, 2134.
(4) Moulton, C. J.; Shaw, B. L. *J. Chem. Soc., Chem. Commun.* **1976**, 365.
(5) Yoshida, T.; Yamagata, T.; Tulip, T. H.; Ibers, J. A.; Otsuka, S. *J. Am. Chem. Soc.* **1978**, *100*, 2063.
(6) Green, M.; Howard, J. A. K.; Spencer, J. L.; Proud, J.; Stone, F. G. A.; Tsipis, C. A. *J. Chem. Soc., Chem. Commun.* **1976**, 671.
(7) Minghetti, G.; Banditelli, G.; Bandini, A. L. *J. Organomet. Chem.* **1977**, *139*, C80.
(8) Brown, M. P.; Puddephatt, R. J.; Rashidi, M.; Seddon, K. R. *Inorg. Chim. Acta* **1977**, *23*, L27; *J. Chem. Soc., Dalton Trans.* **1978**, 516.
(9) (a) Bracher, G.; Grove, D. M.; Pregosin, P. S.; Venanzi, L. M.; *Angew. Chem.* **1979**, *91*, 169; *Angew. Chem., Int. Ed. Engl.* **1979**, *18*, 155. (b) Bracher, G.; Grove, D. M.; Venanzi, L. M.; Bachechi, F.; Mura, P.; Zambonelli, L. *Angew. Chem.* **1978**, *17*, 778; *Angew. Chem., Int. Ed. Engl.* **1978**, *17*, 778. (c) Venanzi, L. M. *Coord. Chem. Rev.* **1982**, *43*, 251-274.
(10) Tulip, T. H.; Yamagata, T.; Yoshida, T.; Wilson, R. D.; Ibers, J. A.; Otsuka, S. *Inorg. Chem.* **1979**, *18*, 2239.
(11) Minghetti, G.; Bandini, A. L.; Banditelli, G.; Bonati, F. *J. Organomet. Chem.* **1979**, *179*, C13.
(12) (a) Brown, M. P.; Fisher, J. R.; Manojlovic-Muir, L. J.; Muir, K. W.; Puddephatt, R. J.; Thomson, M. A.; Seddon, K. R. *J. Chem. Soc., Dalton Trans.* **1979**, 931. (b) Brown, M. P.; Fisher, J. R.; Puddephatt, R. J.; Seddon, K. R. *Inorg. Chem.* **1979**, *18*, 2808. (c) Brown, M. P.; Fisher, J. R.; Mills, A. J.; Puddephatt, R. J.; Thomson, M. A. *Inorg. Chim. Acta* **1980**, *44*, L271. (d) Brown, M. P.; Fisher, J. R.; Hill, R. H.; Puddephatt, R. J.; Seddon, K. R. *Inorg. Chem.* **1981**, *20*, 3516. (e) Hill, R. H.; Puddephatt, R. J. *Inorg. Chim. Acta* **1981**, *54*, L277. (f) Puddephatt, R. J.; Thomson, M. A. *Inorg. Chem.* **1982**, *21*, 75. (g) Frew, A. A.; Hill, R. H.; Manojlovic-Muir, L. J.; Muir, K. W.; Puddephatt, R. J. *J. Chem. Soc., Chem. Commun.* **1982**, 198.
(13) Manojlovic-Muir, L. J.; Muir, K. W. *J. Organomet. Chem.* **1981**, *219*, 129.
(14) Foley, H. C.; Morris, R. H.; Targos, T. S.; Geoffroy, G. L. *J. Am. Chem. Soc.* **1981**, *103*, 7337-7339.

0020-1669/83/1322-2324$01.50/0

Scheme I

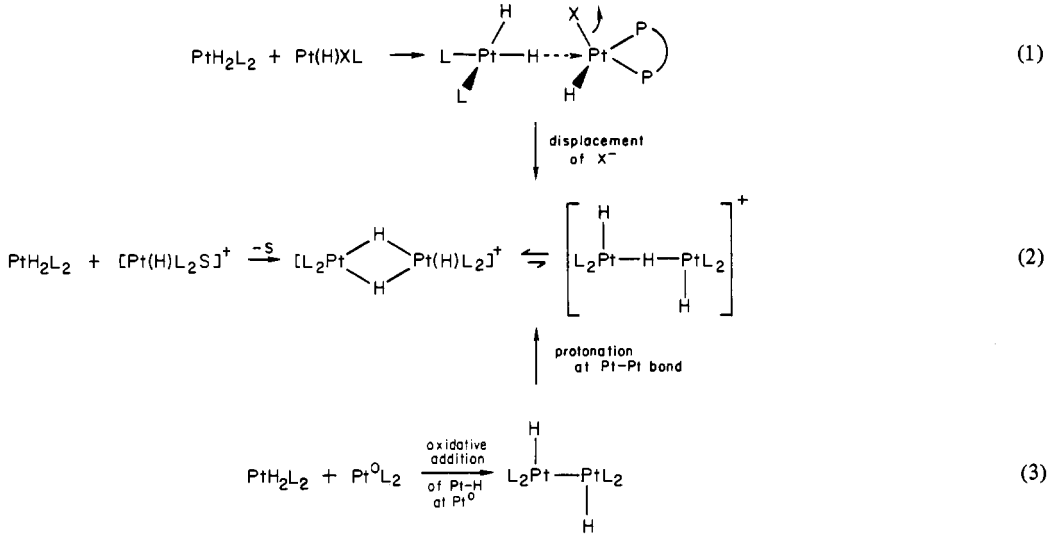

Table I. Analytical[a] and Related[b-d] Data

compd	dec pt/°C	% C	% H	% P	% Pt	% other				ν(Pt-H)/cm^{-1} [e]
$[Pt_2H_3(dpe)_2][BF_4]$ (**1a**)	180	49.00 (48.93)	4.07 (4.00)	9.71 (9.70)	30.58 (30.57)	B	0.90 (0.84)	F	6.36 (5.95)	2000 w, br (Nujol) 2008 s ($CHCl_3$) R: 2030 w, v br[f]
$[Pt_2H_3(dpe)_2][I]$ (**1b**)	110	47.30 (47.44)	4.00 (3.87)	9.39 (9.41)	...	I	10.31 9.64		...	2000 w, br (Nujol)
$[Pt_2H_3(dpe)_2][NO_3]$ (**1c**)	160	49.83 (49.90)	4.14 (4.07)	...	...	N	0.97 (1.12)	O	3.94 (3.84)	2000 w, br (Nujol)
$[Pt_2H_3(dpe)_2][BPh_4]$ (**1d**)	170	60.0 (60.5)	4.60 (4.71)	...	25.70 (25.86)		...		...	2020 m (Nujol)
$[Pt_2D_3(dpe)_2][BF_4]$ (**1a-d_3**)		46.74 (48.8)	3.70 (4.00)							R: 1460 br[g]
$[Pt_2H_3(dpp)_2][BF_4]$ (**2a**)	200	49.65 (49.72)	4.20 (4.22)	...	28.70 (29.91)		...	F	5.62 (5.83)	2010 w, br (Nujol) 2020 s ($CHCl_3$)
$[Pt_2H_3(dpb)_2][BF_4]$ (**3a**)	175	50.29 (50.48)	4.53 (4.43)	...	...		...		...	1975 s, br (Nujol)
$[Pt_2H_3(dpb)_2][NO_3]$ (**3c**)	155	50.18 (51.43)	4.30 (4.51)	...	...	N	1.07 (1.07)		...	1975 s, br (Nujol)
$[Pt_2H_3(dpet)_2][BF_4]$ (**4a**)	215	49.18 (49.08)	3.85 (3.69)							1990 m (Nujol)
$[Pt_2H_3(dpae)_2][BF_4]$ (**5a**)	180	44.70 (45.71)	3.43 (3.73)		27.5 (28.56)			F	5.44 (5.56)	2060 w, br (Nujol) 2060 s ($CHCl_3$)

[a] Calculated values in parentheses. [b] Decomposition point (dec pt) is *above* value cited. [c] Molecular weight of **1a** 1337 in $CHCl_3$ (calcd 1276.4). [d] Λ_M (Ω^{-1} cm^2 mol^{-1}) in acetone: **1a**, 135 (23 °C); **1b**, 110 (20 °C); **1d**, 99 (16 °C); **5a**, 142 (27 °C). [e] IR spectrum unless designated by R (for Raman spectrum of the powdered solid). s = strong, m = medium, w = weak, v = very, br = broad. [f] ν(Pt-(μ-H)-Pt) 700 cm^{-1} br. [g] ν(Pt-(μ-D)-Pt) 400 cm^{-1} br.

More recently, an array of species of higher nuclearity has been obtained, e.g. $[Pt_3H_x(L\text{-}L)_3]^+$ (L-L = dpe, dpae),[15] $[Pt_5H_8(P\text{-}t\text{-}Bu_2Ph)_5]$,[16] $[Pt_3H_6(P\text{-}t\text{-}Bu_3)_3]$, $[Pt_4H_2(P\text{-}t\text{-}Bu_3)_4]$, and $[Pt_4H_8(PPr_2Ph)_4]$.[17] It thus seems that the dinuclear and more generally polynuclear platinum hydrides comprise a class of compounds that is rapidly expanding.

Following our preliminary communication,[7] we report here the syntheses and spectra of a series of cations $[Pt_2H_3(L\text{-}L)_2]^+$ where L-L is a chelating group 5B ligand (P or As), together with the crystal and molecular structure of the salt $[Pt_2H_3(dpe)_2][BPh_4]$.

Results

Syntheses. The dinuclear trihydrido complexes $[Pt_2H_3(L\text{-}L)_2][A]$ that we studied in this work were obtained by the reactions shown in Scheme II. Physical properties and analytical data for the new compounds are summarized in Table I; NMR data, in Table II. In both of the pathways shown in Scheme II, the KBH_4:Pt salt ratio is critical (see Experimental Section). An excess of KBH_4 gives byproducts of higher nuclearity, e.g. $[Pt_3H_x(L\text{-}L)_3]^+$.[15]

Scheme II

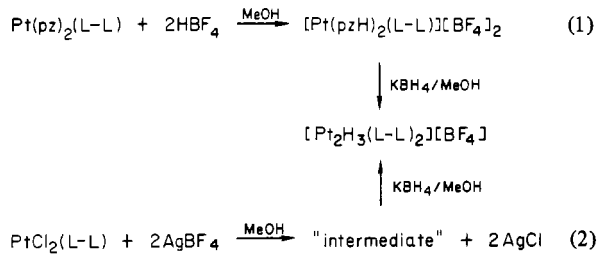

pzH = 3,5-dimethylpyrazole
(1) L-L = dpe, dpp, dpb, dpet, dpae
(2) L-L = dpe, dpp, dpb

(15) Minghetti, G.; Bandini, A. L.; Banditelli, G.; Bonati, F. *J. Organomet. Chem.* **1981**, *214*, C50.
(16) Gregson, D.; Howard, J. A. K.; Murray, M.; Spencer, J. L. *J. Chem. Soc., Chem. Commun.* **1981**, 716.
(17) Frost, P. W.; Howard, J. A. K.; Spencer, J. L.; Turner, D. G.; Gregson, D. *J. Chem. Soc., Chem. Commun.* **1981**, 1104.

Table II. NMR Spectra

		^{1}H (hydride region)			^{31}P{^{1}H}				
compd	solvent	$\delta^{a,b}$	^1J(Pt,H)	^2J(P,H)	δ^a	^1J(Pt,P)	^3J(Pt,P)	^4J(P,P)	^2J(Pt,Pt)
1a	$CDCl_3$	−2.8 qq	500	40.8	57.2	2925	171	9.8	793
1d	CD_2Cl_2	−2.7 qq	503	40					
2a	$CDCl_3$	−3.7 qq	458	40	9.0	2913	172	7.3	
3a	CD_2Cl_2	−4.3 qq	448	40	22.9	3044	188	9.8	
4a	CD_2Cl_2	−2.8 qq	512	42	69.8	2921	177	9.8	
5a	$CDCl_3$	−4.4 qt	552	32.4	63.6	3565	330	28	

[a] In ppm (+) downfield from Me_4Si (^{1}H) and H_3PO_4 (^{31}P); J in Hz. [b] t = triplet, q = quintet.

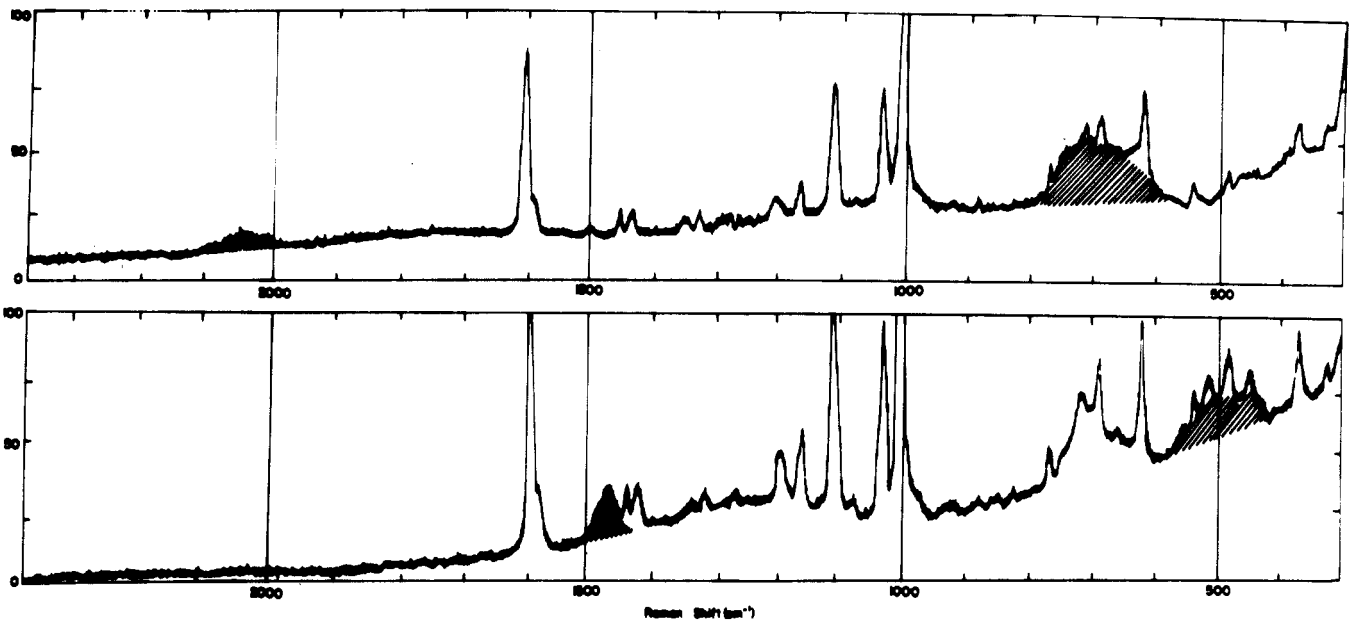

Figure 1. Raman spectra (solid state): upper trace, $[Pt_2H_3(Ph_2P(CH_2)_2PPh_2)_2][BF_4]$ (**1a**); lower trace, $[Pt_2D_3(Ph_2P(CH_2)_2PPh_2)_2][BF_4]$ (**1a**-d_3).

The "intermediate" in reaction 2 of Scheme II may be a dinuclear cationic complex of the type $[(Pt(L\text{-}L))_2(\mu\text{-}OR)_2]^{2+}$ or, in solution, a mononuclear complex of the type $[Pt(OR)(S)(L\text{-}L)]^+$ (S = solvent).

Most of the complexes **1–5** have been isolated as the tetrafluoroborate salts from which the other salts are obtained by metathesis reactions with KI, KNO_3, or $KBPh_4$, respectively. All the complexes are air-stable, crystalline solids, soluble in acetone or dichloromethane. Upon prolonged standing in chlorinated solvents, however, they are found to decompose somewhat, affording uncharacterized products in which it is likely that the hydrido hydrogen atoms are partially replaced by chlorine atoms.

Spectra. Complexes **1–5** show a broad band in the IR spectra around 2000 cm^{-1} both in solution and in the solid state. This is assigned to a Pt–H (terminal) stretching mode, ν(Pt–H). No absorption due to a bridging hydride is observed.[10,18] Assignment of the terminal stretching mode is confirmed by disappearance of the band in the deuterated species, **1a**-d_3. The corresponding ν(Pt–D) is not detected because the region in which it is expected is obscured by absorptions due to the diphosphine ligands. The high value of ν(Pt–H) suggests a rather strong Pt–H (terminal) bond, in agreement with a trans P–Pt–H arrangement.

The Raman spectrum of **1a** is shown in Figure 1, upper trace. This contains a weak band centered at 2040 cm^{-1}, which is observed to shift to 1470 cm^{-1} in the deuterated analogue, lower trace, Figure 1. The ν(Pt–D) band is shifted by the expected amount (ν(Pt–H)/ν(Pt–D) = 1.39) and is significantly less broad as also expected.[19]

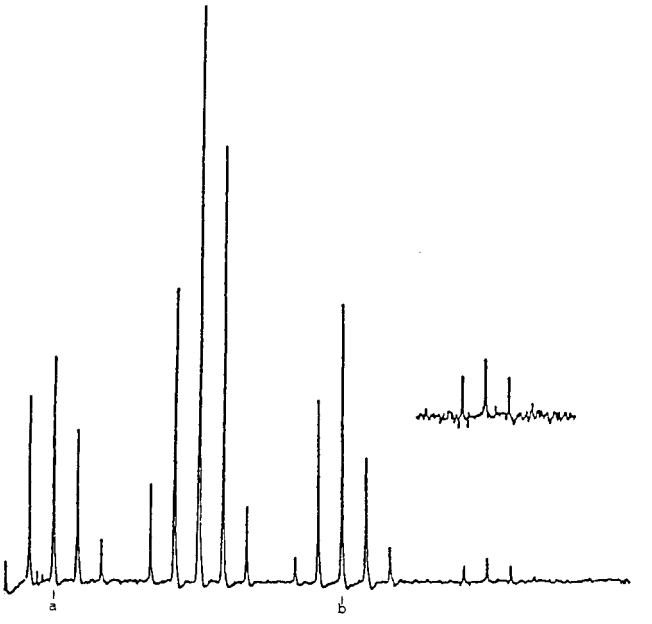

Figure 2. ^{1}H NMR (100 MHz, 25 °C, $CDCl_3$ solution) high-field region for $[Pt_2H_3(Ph_2P(CH_2)_2PPh_2)_2][BF_4]$ (**1a**). Separation of peaks a and b is 500 Hz.

^{1}H NMR spectra of complexes **1–4** show a quintet of binomial quintets centered around δ −2.7 to −4.3; see Figure 2 and Table II. Part of the lowest field quintet is obscured by the signals of the ligands. This pattern indicates fluxional behavior for the molecules and averaging, which persists in

(18) Ciriano, M.; Green, M.; Howard, J. A. K.; Proud, J.; Spencer, J. L.; Stone, F. G. A.; Tsipis, C. A. *J. Chem. Soc., Dalton Trans.* **1978**, 801.

(19) Saillant, R. B.; Kaesz, H. D. *Chem. Rev.* **1972**, *72*, 231.

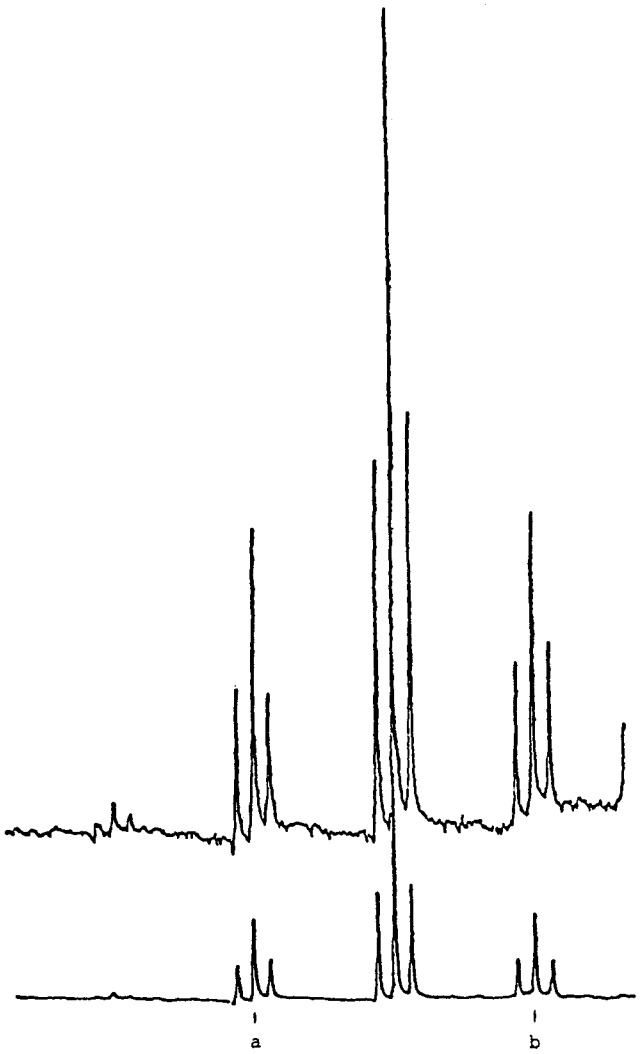

Figure 3. ^{1}H NMR (100 MHz, 25 °C, $CDCl_3$ solution) high-field region for $[Pt_2H_3(Ph_2P(CH_2)_2AsPh_2)_2][BF_4]$ (**5a**). Separation of peaks a and b is 552 Hz.

all the species down to ca. −60 °C ($CDCl_3$ solution) or even down to −95 °C for complex **1a** ($(CD_3)_2C{=}O$ solution) and for **3a** and **4a** (CD_2Cl_2 solution). The splitting of the signal into a quintet is a consequence of the existence in the dinuclear systems of three isotopomers, namely $P_2Pt{-}PtP_2$ (43.8%), $P_2Pt{-}^{195}PtP_2$ (44.8%), and $P_2{}^{195}Pt{-}^{195}PtP_2$ (11.4%) (where ^{195}Pt is the isotope with $I = {}^1/_2$ in 33.8% abundance and Pt represents all the other isotopes with $I = 0$). These isotopomers are present in the approximate ratio of 4:4:1 and give rise respectively to a singlet, a doublet, and a triplet in the ^{1}H resonances. The superposition of the three subspectra appears as a quintet of relative intensity 1:8:18:8:1, where the signals are separated by ${}^1/_2(^1J(Pt,H))$. Each signal is further split into a binomial quintet by coupling to four phosphorus nuclei, $^2J(P,H)$, which are therefore chemically and magnetically equivalent in any of the isotopomers. Similarly, in the case of complex **5a** where L-L is dpae, $Ph_2P(CH_2)_2AsPh_2$, each signal of the quintet is split into a binomial triplet by coupling to two equivalent phosphorus atoms (Figure 3). The $^{31}P\{^1H\}$ and $^{195}Pt\{^1H\}$ spectra are also fully in agreement with the presence of two equivalent platinum and four equivalent phosphorus nuclei.

The observed and simulated spectra of **1a** are shown in Figure 4. Once again, the spectrum results from superposition of the subspectra of the three isotopomers: in the $^{31}P\{^1H\}$ spectra, the $P_2Pt{-}PtP_2$ species gives a single line while the $P_2Pt{-}^{195}PtP_2$ species gives a first-order spectrum composed of two doublets, one due to coupling to ^{195}Pt of the two phosphorus atoms which are bonded to it, $^1J(Pt,P)$, and one due to coupling of the two far phosphorus atoms, $^3J(Pt,P)$. Each signal is further split into binomial triplets by coupling with the other two nonequivalent phosphorus atoms, $^4J(P,P)$. The spectrum of the third isotopomer, $P_2{}^{195}Pt{-}^{195}PtP_2$, is more complicated and is essentially characterized by a doublet separation, $^1J(Pt,P) + {}^3J(Pt,P)$, both constants having the same sign. The full analysis of this spectrum, which has been previously described in detail by Otsuka et al.,[10] allows us to establish, inter alia, the $^2J(Pt,Pt)$ value in complex **1a**. By means of the parameters $^1J(Pt,P)$, $^3J(Pt,P)$, $^4J(P,P)$, and $^2J(Pt,Pt)$ (see Table II), the $^{31}P\{^1H\}$ and $^{195}Pt\{^1H\}$ spectra have been simulated to a very good fit between computed and observed spectra.

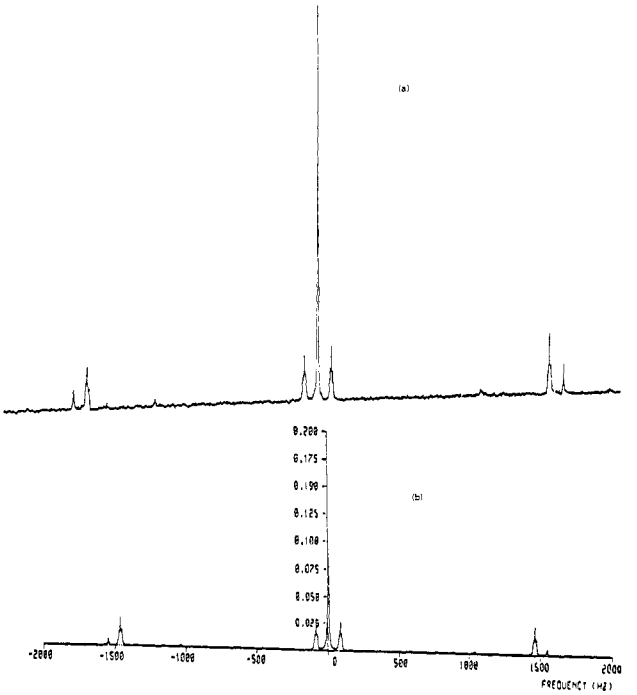

Figure 4. (a) $^{31}P\{^1H\}$ NMR spectrum (25 °C, $CDCl_3$ solution) for $[Pt_2H_3(Ph_2P(CH_2)_2PPh_2)_2][BF_4]$ (**1a**). (b) Computer simulation.

In the non-H-decoupled ^{195}Pt spectrum of **1a**, all the peaks observed in the $^{195}Pt\{^1H\}$ spectrum become split into quartets ($^1J(Pt,H) = 500$ Hz; see Figure 5c, central peak at 591 ppm). The number of equilibrating hydrido hydrogen atoms is thus established unequivocally to be 3. The same result, on the other hand, had been independently reached by integration of the ^{1}H NMR against an internal standard ($4\text{-}NO_2C_6H_4OCH_3$) or even by the chemical method involving displacement of hydrogen by iodine. The observed values of $^1J(Pt,H)$ and $^2J(P,H)$ require some comment. The values $^1J(Pt,H)$ in the range 448–552 Hz are quite small when contrasted with those observed for terminal hydrides[20] but are in line with values obtained in other platinum complexes with bridging hydride(s).[7-9a,10,19] As previously observed,[21] a decrease in the $^1J(Pt,H)$ values is found on going from a five-membered ring to a six- or seven-membered ring, suggesting that the s character of the bonding orbitals of platinum gradually decreases as the ring size increases. The $^2J(P,H)$ values of ca. 40 Hz are intermediate between the values usually found in the square-planar platinum(II) complexes in trans P–Pt–H (>100 Hz) and cis P–Pt–H (<25 Hz) arrangements in agreement with a $(\mu\text{-H})_3$ structure.

(20) Reference 2, pp 50–60.
(21) Yoshida, T.; Yamagata, T.; Tulip, T. H.; Ibers, J. A.; Otsuka, S. *J. Am. Chem. Soc.* **1978**, *100*, 2064.
(22) Jesson, J. P. In "Transition Metal Hydrides"; Muetterties, E. L., Ed.; Marcel Dekker: New York, 1971.

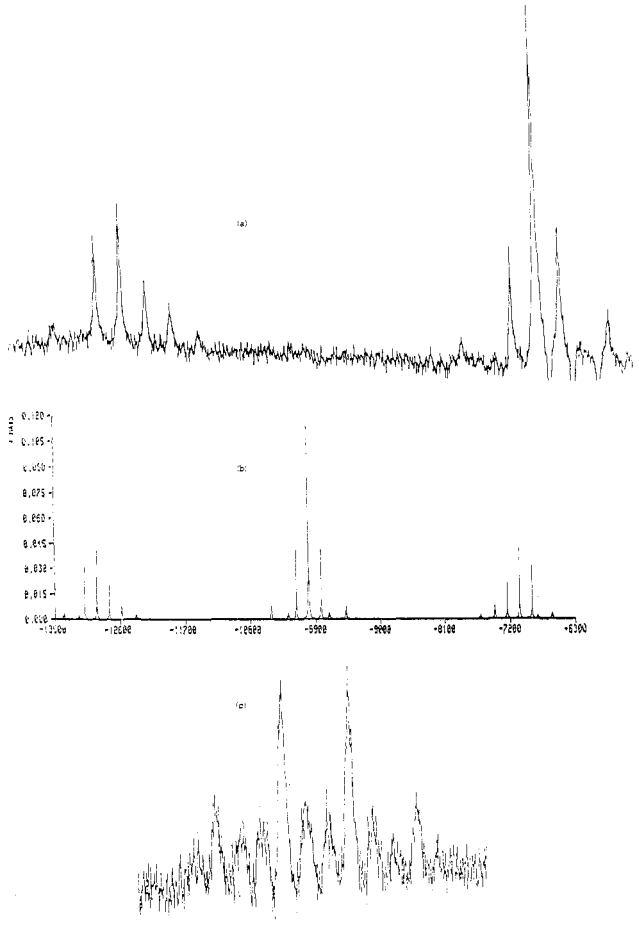

Figure 5. (a) Central peak and low-field satellites in the $^{195}Pt\{^1H\}$ NMR spectrum (25 °C, $CDCl_3$ solution) for $[Pt_2H_3(Ph_2P(CH_2)_2PPh_2)_2][BF_4]$ (**1a**). (b) Computer simulation. (c) Non-H-decoupled spectrum. The central peak is at −591 ppm. The separation in the peaks of the quartet is $^1J(Pt,H)$ 500 Hz.

In conclusion, while the spectroscopic data rule out a $(\mu\text{-H})_3$ structure, they do not allow us to distinguish unambiguously between the mono- or di-hydrogen-bridged structures shown at the top of Scheme I. These facts and the novel aspects of these dinuclear species prompted us to undertake the structural studies that are described in the latter part of the Experimental Section and the discussion that follows.

Experimental Section

The chelating ligands, dpe, dpp, dpb, dpet, and dpae, were purchased from Strem Chemicals; KBH_4, $NaBD_4$, and $AgBF_4$ were obtained from Fluka. These were used without further purification. The starting platinum complexes $[Pt(pz)_2(L\text{-}L)]$ and $[Pt(pzH)_2(L\text{-}L)]^{2+}$ (pzH = 3,5-dimethylpyrazole) were prepared from $PtCl_2(L\text{-}L)$, as previously described.[7]

Analyses were performed by the microanalytical laboratory of the University of Milan and by Dr. F. Pascher, Mikroanalytisches Laboratorium, Bonn, West Germany.

Spectra were obtained as follows: IR, Beckman 4210; Raman, Cary 81 equipped with a Spectra-Physics 125 He/Ne laser (15 803-cm^{-1} exciting line); ^1H and $^{31}P\{^1H\}$ NMR, Varian XL 100 and XL 200, Bruker WP 80 (32.4 MHz). ^{31}P chemical shifts are reported in parts per million, relative to external 85% H_3PO_4, *upfield* being *negative*. The ^{195}Pt spectra were recorded on a JEOL PS-100 spectrometer (21 MHz): the standard frequency is taken as 21.4 MHz when the proton resonance of internal Me_4Si is at 100 MHz. Positive shifts are to high frequency.

Preparation of the $[Pt_2H_3(L\text{-}L)_2]^+$ Complexes. Method I (See Eq 1, Scheme II). Complexes **1a**, **2a**, **3a**, and **4a** were obtained as the BF_4^- salts by reaction of $[Pt(pzH)_2(L\text{-}L)][BF_4]_2$[23] with KBH_4 (BH_4:Pt molar ratio 1:1) in methanol. In a typical experiment, 1.0 mmol of finely ground KBH_4 dissolved in 30 mL of freshly distilled methanol is added to a solution of the platinum complex (1.0 mmol in ca. 50 mL of methanol). After being stirred for 15 min, the solution is evaporated to dryness and the residue taken up with dichloromethane. To the filtered solution is added diethyl ether to give the crude product, which is crystallized from the solvent mix. Yields: **1a**, ca. 80%; **2a**, 80%; **3a**, 88%; **4a**, 70%. The deuterated analogue **1a**-d_3 is obtained in 70% yield with $NaBD_4$. Yields of **5a** are usually lower, but 65% yield is obtained by using a molar ratio of BH_4^-:Pt of 0.5:1. Other complexes are obtained from the tetrafluoroborate salts by exchange reactions (yields are those of the analytically pure samples recrystallized from CH_2Cl_2/diethyl ether): **1b**, 56% (KI/methanol); **1c**, 43% (KNO_3/methanol); **1d**, 80% ($NaBPh_4$/acetone; **3c**, 73% (KNO_3/methanol).

Method II (See Eq 2, Scheme II) (via Intermediates 1 and 3, L-L = dpe and dpb, Respectively). To a suspension of $PtCl_2(L\text{-}L)$ (6.6 mmol) in 150 mL of MeOH is added a solution of $AgBF_4$ (14 mmol) in 30 mL of MeOH. This is filtered (to remove AgCl) and taken to dryness. The residue is dissolved in CH_2Cl_2, the solution is filtered and evaporated, and the new residue is redissolved in MeOH and precipitated by reduction of solvent volume. Crude product is filtered off and dissolved in CH_2Cl_2, the solution is filtered and taken to dryness, and the solid is recrystallized from MeOH; yield 70%. Intermediate **2**, L-L = dpp, is similarly isolated by treatment of a suspension of $PtCl_2$(dpp) (3.5 g, 5.2 mmol/150 mL of MeOH) with a solution of $AgBF_4$ (2.3 g/50 mL of MeOH). The resulting oily product is stirred overnight under dry Et_2O, forming a white product. An analytically pure sample (80% yield) is obtained by successive steps as above (dissolve in CH_2Cl_2, filter, evaporate to dryness redissolve in MeOH, and precipitate with Et_2O).

Synthesis of **1a** or **2a** occurs by reaction of the intermediates (assumed to be $[Pt_2(OH)_2(L\text{-}L)_2][BF_4]_2$) with KBH_4 (BH_4:Pt molar ratio 1:2). Typically, 0.4 mmol of intermediate in 150 mL of MeOH is added dropwise (under N_2) to a solution of KBH_4 (0.4 mmol/50 mL of MeOH). The resulting yellow solution is evaporated to a small volume to cause precipitation of a yellow solid. Recrystallization twice from CH_2Cl_2/Et_2O yields **1a**, 45%, or **2a**, 63%.

Collection and Reduction of the X-ray Data for 1d, $[Pt_2H_3(dpe)_2][BPh_4]$. A pale yellow crystal of **1d** suitable for diffraction studies was obtained by slow evaporation of an acetone/diethyl ether solution. Preliminary photographic inspection revealed this to belong to the monoclinic system. Systematic extinctions ($h0l$, $h + l = 2n + 1$; $0k0$, $k = 2n + 1$) characteristic of the space group $C_{2h}^5\text{-}P2_1/n$ were observed.

Cell constants were obtained by least-squares refinement of 15 reflections of the crystal centered on a Syntex $P\bar{1}$ diffractometer, $20° < 2\theta < 26°$. These and other crystallographic data are compiled in Table III.

Intensity data were collected by using the $\theta\text{–}2\theta$ scan method. Background counts were measured at each end of the scan range, with both the crystal and the counter held stationary for a total time equal to the scan time. The intensities of three standard reflections were measured after every 97 reflections. These showed no appreciable change during the data collection. The data were processed as previously described, with a p value of 0.04.[24] The data were corrected for Lorentz and polarization effects and for absorption. After the data were processed, 6663 unique reflections having $I > 3\sigma(I)$ were used in subsequent calculations.

Solution and Refinement of the Structure. The Pt atoms were easily located in a three-dimensional Patterson synthesis. Positions of non-hydrogen atoms were obtained by using least-squares refinements and difference Fourier syntheses. The quantity minimized was $\sum w(|F_o| - |F_c|)^2$ where $w = 1/(\sigma^2|F_o|)$.

The scattering factors for neutral Pt, P, N, C, and B were taken from ref 25 while those of H were from Stewart et al.[26] Real and imaginary components of anomalous dispersion for Pt and P were included. The agreement indices for the least-squares refinement are given at the bottom of Table III. Isotropic refinement for all non-

(23) Minghetti, G.; Banditelli, G.; Bonati, F. *J. Chem. Soc., Dalton Trans.* **1979**, 1851.

(24) Andrews, M. A.; Van Buskirk, G.; Knobler, C. B.; Kaesz, H. D. *J. Am. Chem. Soc.* **1979**, *101*, 7245.

(25) "International Tables for X-ray Crystallography"; Kynoch Press: Birmingham, England, 1974; Vol. 4.

(26) Stewart, R. F., Davidson, E. R.; Simpson, W. T. *J. Chem. Phys.* **1965**, *42*, 3175.

Table III. Crystal and Intensity Collection Data for $[Pt_2H_3(Ph_2P(CH_2)_2PPh_2)_2][BPh_4]$

formula	$Pt_2P_4C_{76}BH_{71}$
fw	1509.3
a/Å	11.107 (2)
b/Å	29.118 (4)
c/Å	19.464 (2)
β/deg	97.62 (1)
V/Å^3	6297.0 (1.0)
Z	4
ρ(calcd)/g cm^{-3}	1.59
space group	$C_{2h}^5 - P2_1/n$
cryst size/cm	0.021, 0.0065, 0.03
normals to faces	$0\bar{1}0$, $\bar{1}0\bar{1}$, $\bar{1}\bar{1}3$
temp/K	115
radiat source; λ/Å	Mo Kα (graphite monochromated); 0.71069
abs coeff (μ)/cm^{-1}	46.628
transmissn factors	0.4009–0.7466
scan rate/deg min^{-1}	3
scan range: above Kα_1	1.0
below Kα_2	1.0
bkgd time	=scan time
2θ limits/deg	45
observns	$h,k,\pm l$
tot obsd data	8270
no. of unique data ($I_o > 3\sigma I_o$)	6663
final no. of variables	388
R/%[a]	0.035
R_w/%[b]	0.044
error in observn of unit wt	1.4527

[a] $R = \Sigma||F_o| - |F_c||/\Sigma|F_o|$. [b] $R_w = [\Sigma w(|F_o| - |F_c|)^2/\Sigma wF_o^2]^{1/2}$, $w = 1/(\sigma^2|F_o|)$.

hydrogen atoms resulted in an agreement index $R = 0.0868$. Refinement of 388 parameters included positional and anisotropic thermal parameters for Pt, P, B, and methylene C and positional and isotropic thermal parameters for phenyl C, methylene H, and phenyl H in calculated positions with assigned thermal parameters. This refinement led to values of R, R_w, and goodness of fit (GOF) of 0.035, 0.045, and 1.4786, respectively.

At this point two difference maps were calculated, one using all the observed data and the second using data to a maximum $(\sin\theta)/\lambda$ of 0.35. A description of the difference peaks is given with use of the numbering scheme in the ORTEP diagram shown in Figure 6. In the first map, the highest of the top five difference peaks is seen bridging Pt(1)–Pt(2) trans to P(3); the third highest peak is terminal on Pt(1) trans to P(2) while the fifth highest peak is bridging Pt(1)–Pt(2) trans to P(4). The remaining two difference peaks are within 1.1 Å of Pt(1) or Pt(2). In the second map the lower of the two nonhydride peaks is 1.2 Å from P(3) and the higher is 0.9 Å from Pt(1). With all other parameters used for structure factor calculations only, the scale factor and the positions of the three hydride difference peaks were allowed to vary on the basis of data having $(\sin\theta)/\lambda < 0.35$. Although the locations cannot be very accurate, these positional parameters do settle after five cycles of refinement: 10 parameters, 1978 reflections, $R = 0.03$, $R_w = 0.04$, GOF = 1.5325 with shifts for three hydride atoms 0.009, 0.03, and 0.05 Å (errors 0.1 Å). The approximate locations of the hydrogen atoms have been confirmed through an independent neutron diffraction study.[27] The present work and its companion paper describing the synthesis and structure determination of $[Pt_2(\mu\text{-}H,\mu\text{-}CO)(Ph_2P(CH_2)_2PPh_2)_2][BF_4]$[28] constitute the first location of bridging hydrogens in polynuclear platinum derivatives.

The three hydride atoms were then included, for structure factor calculations only, in refinement of the original 388 parameters with all the data (6663 reflections). After two cycles of refinement for convergence, $R = 0.035$, $R_w = 0.044$, and GOF = 1.4527. Positional parameters of the Pt atoms and the principal atoms in their coordination spheres are given in Table IV; anisotropic thermal parameters are given in Table A (supplementary material). Phenyl group carbon atom positional and isotropic thermal parameters are given in Supplemental Table B while the derived phenyl group hydrogen atom positions are given in Supplementary Table C. A tabulation of calculated and observed structure factors is also available in the supplementary material.

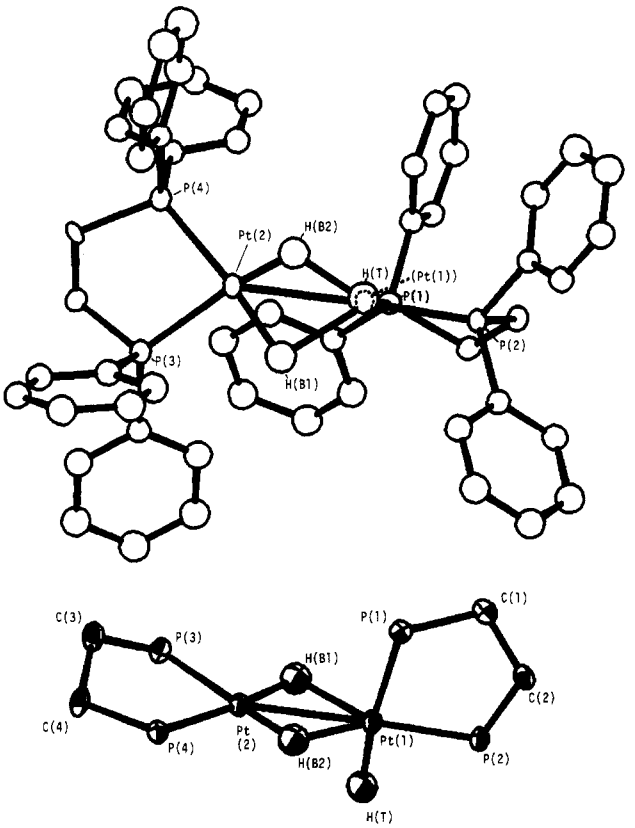

Figure 6. ORTEP projections of the cation in $[Pt_2H_3(Ph_2P(CH_2)_2PPh_2)_2][BPh_4]$ (1d). Upper projection looks down along the H(T)–Pt(1) vector, Pt(1) being eclipsed by H(T). Lower projection shows cation rotated by 90° from its position in the upper projection.

Table IV. Positional Parameters (in Fractional Coordinates) for 1d[a]

atom	x	y	z
B(001)	0.5334 (8)	0.1946 (3)	−0.4067 (5)
C(001)	0.3120 (7)	0.0700 (2)	−0.3124 (4)
C(002)	0.2728 (7)	0.1178 (2)	−0.2902 (4)
C(003)	0.0020 (7)	−0.1480 (2)	−0.1576 (4)
C(004)	−0.1234 (7)	−0.1295 (2)	−0.1500 (4)
P(1)	0.1892 (2)	0.0300 (1)	−0.2995 (1)
P(2)	0.2318 (2)	0.1144 (1)	−0.2019 (1)
P(3)	0.1142 (2)	−0.1059 (1)	−0.1205 (1)
P(4)	−0.1363 (2)	−0.0717 (1)	−0.1878 (1)
Pt(1)	0.14729 (3)	0.046056 (9)	−0.18954 (1)
Pt(2)	0.04829 (3)	−0.037104 (4)	−0.16519 (1)
H(T)[b]	0.1153	0.0639	−0.1211
H(B1)[b]	0.1937	−0.0167	−0.1470
H(B2)[b]	0.0221	0.0084	−0.1852

[a] Estimated standard deviation of the least significant digit is given in parentheses. Derived or group atom positions (phenyl hydrogen and phenyl carbon atoms) are given as supplementary material. [b] Positional parameters (not refined) are given for terminal and bridging hydrogen atoms in the coordination sphere of the Pt atoms.

Description of the Structure

The crystal consists of discrete cations and anions. The overall geometry of the cation and the system used in labeling the principal atoms are shown in Figure 6. Selected bond distances and angles are presented in Table V.

Interion Contacts. The ions are well separated in the crystal. A stereoscopic drawing showing the packing of both cations

(27) Bau, R.; Koetzle, T., private communication, manuscript in preparation.
(28) Minghetti, G.; Bandini, A. L.; Banditelli, G.; Bonati, F.; Szostak, R.; Strouse, C. E.; Knobler, C. B.; Kaesz, H. D. *Inorg. Chem.*, following paper in this issue.

Table V. Principal Interatomic Distances (Å) and Angles (deg) in **1d**[a]

Distances

P(1)-Pt(1)	2.317 (2)	Pt(1)-H(T)	1.527	Pt(2)-H(B2)	1.402	C(002)-P(2)	1.853 (7)
P(2)-Pt(1)	2.228 (2)	Pt(1)-H(B2)	1.782	Pt(2)-H(B1)	1.713	C(003)-C(004)	1.519 (11)
P(3)-Pt(2)	2.269 (2)	Pt(1)-H(B1)	2.046	C(001)-C(002)	1.538 (10)	C(003)-P(3)	1.830 (7)
P(4)-Pt(2)	2.274 (2)	Pt(1)-Pt(2)	2.728 (1)	C(001)-P(1)	1.835 (7)	C(004)-P(4)	1.840 (7)

Angles

H(T)-Pt(1)-H(B2)	83.86	H(B1)-Pt(2)-P(3)	88.79	C(031)-P(2)-Pt(1)	120.51 (24)
H(T)-Pt(1)-H(B1)	91.08	H(B1)-Pt(2)-P(4)	174.05	C(002)-P(2)-Pt(1)	107.95 (23)
H(T)-Pt(1)-P(2)	86.72	H(B1)-Pt(2)-Pt(1)	48.53	C(051)-P(3)-C(061)	106.13 (35)
H(T)-Pt(1)-P(1)	171.43	P(3)-Pt(2)-P(4)	85.49 (7)	C(051)-P(3)-C(003)	105.59 (35)
H(T)-Pt(1)-Pt(2)	90.06	P(3)-Pt(2)-Pt(1)	137.27 (5)	C(051)-P(3)-Pt(2)	111.18 (25)
H(B2)-Pt(1)-H(B1)	65.60	P(4)-Pt(2)-Pt(1)	137.09 (5)	C(061)-P(3)-C(003)	103.83 (35)
H(B2)-Pt(1)-P(2)	153.89	Pt(2)-H(B1)-Pt(1)	92.60 (2)	C(061)-P(3)-Pt(2)	123.00 (25)
H(B2)-Pt(1)-P(1)	100.09	Pt(2)-H(B2)-Pt(1)	117.45 (2)	C(003)-P(3)-Pt(2)	105.66 (25)
H(B2)-Pt(1)-Pt(2)	27.13	C(021)-P(1)-C(011)	104.91 (33)	C(071)-P(4)-C(081)	105.47 (35)
H(B1)-Pt(1)-P(2)	139.04	C(021)-P(1)-C(001)	101.72 (33)	C(071)-P(4)-C(004)	104.34 (34)
H(B1)-Pt(1)-P(1)	97.47	C(021)-P(1)-Pt(1)	114.69 (25)	C(071)-P(4)-Pt(2)	117.24 (24)
H(B1)-Pt(1)-Pt(2)	38.87	C(011)-P(1)-C(001)	105.93 (34)	C(081)-P(4)-C(004)	107.67 (34)
P(2)-Pt(1)-P(1)	86.50 (7)	C(011)-P(1)-Pt(1)	123.02 (25)	C(081)-P(4)-Pt(2)	113.55 (25)
P(2)-Pt(1)-Pt(2)	176.16 (5)	C(001)-P(1)-Pt(1)	104.21 (24)	C(004)-P(4)-Pt(2)	107.86 (25)
P(1)-Pt(1)-Pt(2)	96.90 (5)	C(041)-P(2)-C(031)	103.88 (33)	C(002)-C(001)-P(1)	106.94 (50)
H(B2)-Pt(2)-H(B1)	83.40	C(041)-P(2)-C(002)	106.34 (34)	C(001)-C(002)-P(2)	109.34 (47)
H(B2)-Pt(2)-P(3)	170.90	C(041)-P(2)-Pt(1)	114.59 (24)	C(004)-C(003)-P(3)	107.95 (52)
H(B2)-Pt(2)-P(4)	102.43	C(031)-P(2)-C(002)	102.14 (32)	C(003)-C(004)-P(4)	107.96 (51)
H(B2)-Pt(2)-Pt(1)	35.42				

[a] No esd given for distances and angles involving H(T), H(B1), and H(B2), whose positions were not refined. For other data, the esd of the least significant digit is given in parentheses.

and anions is given in Supplemental Figure A. The closest *non*-hydrogen atom contact between cation and anion is 3.46 Å (between atoms C(83) and C(114)). A stereoscopic drawing showing the packing of the cations alone is given in Supplemental Figure B. The closest *non*-hydrogen atom contact between cations is 3.42 Å (between atoms C(52) and C(73)). A stereoscopic drawing showing the packing of the anions alone is given in Supplemental Figure C. The closest *non*-hydrogen atom contact between anions is greater than 3.5 Å.

The Tetraphenylborate Anion. The numbering scheme used is

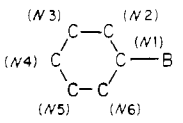

$N = 9\text{-}12$

The anion exhibits the usual distortions from ideal geometry.[7,29] The B–C bond lengths are equivalent and average to 1.65 (4) Å, in agreement with other reported values in the range 1.66–1.67 Å. The C–B–C bond angles do not deviate greatly from the tetrahedral value, ranging from 107.8 (6) to 111.6 (6)°. The boron atom is displaced an average of 0.10 Å from the planes of the phenyl rings. Similar displacements of 0.12, 0.12, 0.11, and 0.11 Å have been cited previously.

The Dinuclear Cation: Coordination Spheres around the Pt Atoms. The dinuclear cation is shown in Figure 6. The Pt(1)–Pt(2) separation is 2.728 (1) Å, less than 2.765 (1) Å found[21] in $Pt_2((t\text{-}Bu)_2P(CH_2)_3P(t\text{-}Bu)_2)_2$ (**6**) or 2.768 (2) Å found[10] in $[Pt_2H_3((t\text{-}Bu)_2P(CH_2)_3P(t\text{-}Bu)_2)_2][BPh_4]$ (**7**). Other previously reported complexes containing μ-hydrido ligands unaccompanied by other bridging groups show metal–metal separations longer than in analogous unbridged complexes. The majority of Pt–Pt bond lengths are shorter than 2.77 Å. A compilation of such distances has recently been given by Venanzi et al.[30] in a report of the structures of $[(PEt_3)_2Pt(\mu\text{-}H)_2PtY(PEt_3)_2][BPh_4]$ (Y = H, Ph).

Examination of the atoms other than hydrogen in the coordination sphere around each Pt center (i.e., the other Pt and the two P atoms of the chelating ligand) leads to the following observations: Pt(2) is displaced 0.085 Å from the Pt(1)P(1)P(2) plane while Pt(1) is displaced 0.135 Å from the Pt(2)P(3)P(4) plane. The angles formed by the Pt–Pt vector with normals to these planes are respectively 91.8 and 92.8°. Around Pt(1), the P–Pt–P angles are 86.5° while those around Pt(2) are 85.5°. These are much smaller than values found in Pt(II) complexes; see discussion below.

The platinum and the two phosphorus atoms around Pt(2) define a distorted trigonal array. The distances Pt(2)–P(3) and Pt(2)–P(4) as well as the angles P(3)–Pt(2)–Pt(1) and P(4)–Pt(2)–Pt(1) are equal within experimental error: 2.269 and 2.274 (2) Å and 137.27 and 137.09 (5)°, respectively.

The platinum and two phosphorus atoms around Pt(1) are present in an apparent square-planar array where in one of the positions we locate a terminally bonded H atom (see the discussion of assignment of peaks in difference maps, above). In this geometry the Pt(1)–P(1) and Pt(1)–P(2) distances are not equivalent: 2.318 and 2.228 Å, respectively. The shorter separation involves P(2) trans to Pt(2) while the moiety trans to P(1) is assumed to be the terminally bonded H. These effects are also found in the trihydride cation in **7**,[10] whose geometry differs from that of **1d** as discussed in the section that follows.

Comparison of Structure Types for Dinuclear Cations of Platinum. Dinuclear hydrido cationic complexes of the general formula $[Pt_2H_n\text{-}R_{3-n}L_4]^+$[9,10,15,30,31] are heuristically regarded[9c,31] as arising from the interaction of a donor hydride with an acceptor cation (PtH_2L_2 + $[Pt(H)L_2]^+$, Scheme I), a concept earlier suggested for the chemistry and bonding in $(OC)_5Re\text{-}(\mu\text{-}H)\text{-}Re(CO)_4\text{-}cis\text{-}Mn(CO)_5$[32] and further developed in the interpretations of a variety of polynuclear hydride complexes.[33] Using such ideas, we can relate our results with others in this area using the four structures A–D, shown

(29) (a) Cramer, R. E.; Huneke, J. T. *Inorg. Chem.* **1978**, *17*, 365. (b) Duggan, D. M.; Hendrickson, D. N. *Ibid.* **1974**, *13*, 2056. (c) DiVaira, M.; Orlandini, A. B. *J. Chem. Soc., Dalton Trans.* **1972**, 1704.
(30) Bachechi, F.; Bracher, G.; Grove, D. M.; Kellenberger, B.; Pregosin, P. S.; Venanzi, L. M.; Zambonelli, L. *Inorg. Chem.* **1983**, *22*, 1031.
(31) Paonessa, R. S.; Trogler, W. C. *Inorg. Chem.* **1983**, *22*, 1038.
(32) Kaesz, H. D.; Bau, R.; Churchill, M. R. *J. Am. Chem. Soc.* **1967**, *89*, 2775.
(33) Bau, R.; Teller, R. G.; Kirtley, S. W.; Koetzle, T. F. *Acc. Chem. Res.* **1979**, *12*, 176.

Chart I

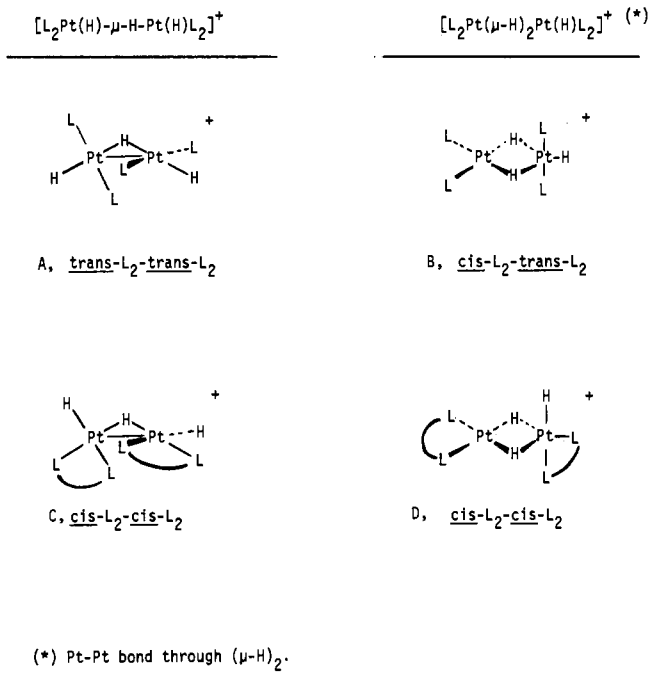

in Chart I. A,[9a,30] C,[10] and D are represented by known structures although only in D (present work and ref 27) have the hydrogen atoms been located. Structure B has been inferred on the basis of NMR data.[31] Of the four permutations of cis and trans orientation of the ligands on the metal centers, only that containing $[Pt(H)\text{-}trans\text{-}L_2\text{-}(\mu\text{-}H)\text{-}Pt(H)\text{-}cis\text{-}L_2]^+$ has not been observed. The most pertinent structural comparison with the present results is to be made with the dinuclear cation in **7**, *i.e.* comparison of structures C and D both with the cis–cis geometry forced by the bidentate chelating ligands. The cation in **7** is believed to have only one hydrogen bridging, as shown in C.[10] In this cation, *both* Pt(L-L) moieties are trigonal, as opposed to trigonal and part of a square-planar arrangement in **1d**, structure D. Furthermore, the Pt–Pt vector in **7** does *not* bisect the P–Pt–P angle in either of the two Pt(L-L) moieties as it does in **1d**. In **7**, the Pt–P separations are 2.342, 2.271 (8) and 2.349, 2.253 Å, with the shorter of these in each pair being the bond that is (nearly) trans to a Pt atom, as observed in **1d**. In **7**, however, the Pt–Pt–P angles involving the shorter Pt–P separations are larger than the Pt–Pt–P angles involving the longer Pt–P separations: 137.3, 120.7° around Pt(1) and 143.6, 116.2(2)° around Pt(2).

We have nothing at present to offer in the way of accounting for such differences except to point out that the cations in **1d** and in **7** are both fluxional on the NMR time scale, exhibiting a very soft potential surface for their conformational changes. Differences in the "bite" angle for the two chelating diphosphines, i.e. $(t\text{-}Bu)_2P(CH_2)_3P(t\text{-}Bu)_2$ as compared to $Ph_2P(CH_2)_2PPh_2$, and/or crystal-packing forces could very well be responsible for structural differences in the solid, which involve small energy changes. In this connection, we wish to point to two recently discovered examples of structure differences in molecules exhibiting low-energy-barrier fluxional behavior, both involving changes in the bonding of carbonyl groups in bridging or "semibridging" positions, namely structural differences observed in the $[Fe(C_5H_5N)_6]^{2+}$ salt[34] as opposed to the $[PPN^+]_2$ salt[35] of $[Fe_4(CO)_{13}]^{2-}$ or in the difference reported between solution- and solid-state structures of $Co_2[\mu\text{-}MeN(P(OMe)_2)_2]_2(CO)_8$.[36]

Acknowledgment. The authors thank Dr. Brian Heaton (University of Kent at Canterbury) for the ^{195}Pt NMR spectra and for simulation of the ^{31}P NMR spectra. We thank Rosemarie Szostak for the Raman spectra.[37] This work was supported by the National Science Foundation (Grant No. 7615436, to H.D.K.), the UCLA Computing Center (in partial support of computational expenses), and the Consiglio Nazionale delle Richerche (CNR), Rome. The Syntex diffractometer was purchased with NSF Grant GP 28248 and the Raman spectrometer with NSF Grant GP 5240.

Supplementary Material Available: Figures A–C, showing stereoscopic projections of the full unit cell, of the cations only, and of the anions only, and Tables A–F, listing anisotropic thermal parameters, positional and isotropic thermal parameters for phenyl group carbon atoms and hydrogen atoms, interatomic distances and angles for the PPh_2 groups and the BF_4^- anion, and calculated and observed structure factors (39 pages). Ordering information is given on any current masthead page.

(34) Doedens, R. J.; Dahl, L. F. *J. Am. Chem. Soc.* **1966**, *88*, 4847.
(35) (a) Knobler, C. B.; Van Buskirk, G.; Kaesz, H. D. "Program and Abstracts", American Crystallographic Association, Calgary, Alberta, Canada, Aug 1980; paper PA19. (b) Van Buskirk, G. Ph.D. Dissertation, University of California, Los Angeles, CA, 1981.
(36) Brown, G. M.; Finholt, J. E.; King, R. B.; Bibber, J. W. *Inorg. Chem.* **1982**, *21*, 2139.
(37) Szostak, R. Ph.D. Dissertation, University of California, Los Angeles, CA, 1981.